Herringbone ordering and lattice distortions in a planar-molecule model for Langmuir monolayers

C. Buzano, A. Pelizzola, and M. Pretti
Istituto Nazionale di Fisica della Materia and Dipartimento di Fisica del Politecnico di Torino, I-10129 Torino, Italy
(Received 22 December 1999; revised manuscript received 23 May 2000)

A model of planar molecules, made up of ''atoms'' interacting by Lennard-Jones potentials and arranged to mimic the cross section of alkyl chains, is used to study the problem of backbone plane ordering in Langmuir monolayers. It is shown that two minima of the interaction energy are reached if molecules lie on the sites of a centered rectangular lattice in a herringbone configuration with two different dihedral angles. These orientationally ordered phases can be related to the so-called herringbone and pseudoherringbone structures, whose lattice distortions qualitatively agree with those determined by means of grazing incidence x-ray diffraction experiments on Langmuir monolayers. A third energy minimum is obtained for a configuration of parallel molecules on an oblique lattice, which has also been observed in some experiments. The competition between the three phases is investigated, upon varying geometric parameters of the model molecules and surface pressure. The effect of temperature is analyzed in a mean field approximation, by taking into account the orientational entropy contribution on a lattice system with variable unit cell parameters. In this framework the transition to an orientationally disordered phase is also pointed out.

PACS number(s): 68.10.−m, 68.15.+e

I. INTRODUCTION

Monolayers of amphiphiles adsorbed at a water-air interface (Langmuir monolayers) have attracted considerable interest, for instance, in biology, where they have been used as simple models of living cell membranes [1], and for their possible future applications, such as the construction of molecular electronic devices based on Langmuir-Blodgett films [2]. The physics of Langmuir monolayers is interesting mainly because they are quasi-two-dimensional systems, which can be used to investigate ordering phenomena and phase transitions in two dimensions. In addition Langmuir monolayers are the only example of two-dimensional systems on which it is possible to perform a direct mechanical compression, which gives rise to peculiar phase transitions [3,4]. The thermodynamic behavior, which is thus controlled by both temperature and surface pressure, turns out to be very rich and displays several condensed phases [5] characterized by different degrees of translational and orientational order. A considerable amount of work has been devoted in recent years to the investigation of phase transitions and structural properties in Langmuir monolayers [6]. Particular attention has been addressed to monolayers composed of the simplest amphiphiles, that is, fatty acids, allowing a detailed determination of the phase diagram [7]. Low temperature phases turn out to be crystalline phases, displaying translational long range order (in one or two directions) with molecules packed in a regular (centered rectangular or distorted hexagonal) lattice, whereas higher temperature phases are mesophases, possessing partial orientational and translational disorder (*hexatic* phases [8]). Moreover, surface pressure drives tilting of molecule long axes, which can take place in different directions (mainly toward nearest neighbors and next nearest neighbors) but usually preserving the symmetry of the rectangular unit cell. Apart from fatty acids, a large number of amphiphiles have also been investigated at the water-air interface [9], even if the phase diagram is not always perfectly known.

In any case an important feature of lower temperature phases is ordering of molecule backbone planes, which usually gives rise, at least in the case of nonchiral (racemic) monolayers, to a herringbonelike structure. If a two-dimensional crystalline phase is considered (namely, CS or L_2'' phases for fatty acids), molecules with opposite backbone orientations are placed on two simple rectangular sublattices, into which the centered rectangular lattice can be split. The ordering of backbone planes can be inferred from knowledge of unit cell parameters, which are usually measured by means of grazing incidence x-ray diffraction (GIXD) experiments [10–12] (see Ref. [6] for a review) and must be analyzed after a projection along the (average) long axes of the molecules, in order to exclude distortions caused by tilt. Recently Kuzmenko, Kaganer, and Leiserowitz [13] have compared projected unit cell parameters extracted from GIXD data on a large variety of amphiphiles (not only fatty acids) in different thermodynamic conditions, showing that in low temperature phases molecules pack with two possible unit cell distortions (toward nearest neighbors and next nearest neighbors), whereas in mesophases the unit cell parameters approach those of a hexagonal lattice with a higher area per molecule. The two different distortions can easily be related to two different packing modes of alkyl chains, which were already characterized several years ago for bulk crystals by Kitaigorodskii [14], on the basis of a simple close packing theory, and can be defined respectively as herringbone (HB) and pseudoherringbone (PHB). Both close packing theory and lattice energy calculations performed by Kuzmenko *et al.* [13] predict that the two packing modes display two different dihedral angles between backbone planes, namely, about 90° for the HB case and about 40° for the PHB case. Obviously neither of these two theories is suitable to reproduce higher temperature (mesophase) behavior, where molecule cross sections are averaged to a circle because of thermal fluctuations, giving rise to a hexagonal unit cell. In the case of chiral monolayers, in which enantiomer separation

takes place, a third packing mode, with molecules arranged on an oblique lattice with parallel backbone planes, has been observed experimentally [15]. The above cited lattice energy calculations [13] partially account for the stability of this configuration and a third energy minimum is actually displayed for zero dihedral angle, even if the rectangular symmetry is imposed and hence no oblique lattice can be observed.

Several models have been proposed in the literature to describe the finite temperature phase behavior of Langmuir monolayers (see Ref. [6]), sometimes reproducing backbone plane ordering, too, and the transition to an orientationally disordered phase. Nevertheless, different packings of the backbones and their relationship with different possible unit cell distortions were usually not taken into account. For example, some molecular dynamics simulations on atomic models [16] have displayed herringbone ordering but have been performed with periodic boundary conditions and a fixed size of the simulation box, thus not allowing distortions to be reproduced. Another approach, particularly devoted to the problem of backbone plane ordering, considers purely two-dimensional models of noncircular particles, representing the projection of amphiphilic molecules in the plane orthogonal to their long axes, and neglects all other degrees of freedom. In this way it has been possible to reproduce, for instance, by means of Monte Carlo simulations [17,18], a phase transition between rotationally ordered and disordered phases, but the fourfold symmetry of the model potential employed did not allow a parallel alignment to be distinguished from a real herringbone ordering, which actually needs a twofold symmetry. A model with such a symmetry, consisting of an effective quadrupole-quadrupole potential, which depends on orientation variables, was developed quite a long time ago by Meyer [19], and subsequently studied by various statistical mechanical techniques [20–27]. For this model the herringbone structure turns out to minimize the energy, if molecules are fixed on a hexagonal lattice, but the effective potential is independent of distance and hence it is not possible to take into account lattice distortions occurring in Langmuir monolayers. More recently Schofield and Rice have considered the problem of backbone ordering by means of a lattice density functional theory [28], whereas Swanson, Luty, and Eckhardt have employed an atomic model of molecules, calculating the energy of the uniformly strained lattice (which allows them to take into account backbone packings) and hence evaluating the partition function by integrating over the strains [29].

In this paper we shall approach the problem of unit cell distortions on the basis of a planar-molecule model, which is intended to exclude tilt effects and describe the monolayer in the plane orthogonal to the tilt direction, as in Refs. [17,18]. Unlike that case, a particular (rotationally twofold symmetric) shape of model molecules is chosen, which tries to mimic the cross section of alkyl chains and turns out to be an important ingredient in reproducing backbone plane ordering with the different packing modes. The molecules have continuous rotational degrees of freedom and the possibility of unit cell distortions is taken into account in the following way. Unit cell parameters are calculated by finding the packing mode that minimizes the free energy, which is evaluated in a mean field approximation, introducing the orientational entropy contribution. The paper is organized as follows. In Sec. II we give a description of the proposed model, starting from molecule features, which are justified on the basis of qualitative arguments about the structure of alkyl chains. Assuming a Lennard-Jones potential to describe interaction between the elementary constituents of the model molecules, the total interaction energy of the model is derived. In Sec. III we show that a stationary point of the energy is reached if molecules are arranged on a generic two-dimensional Bravais lattice split into four sublattices on which molecules must have the same orientations, to be determined by means of a variational procedure (the detailed proof, together with a method to verify that the stationary point is actually a minimum, is presented in an Appendix). A ground state analysis is then performed, upon varying a geometrical parameter that characterizes model molecules, by carrying out a (numerical) variational procedure, which also returns the optimal lattice parameters. These calculations actually show three different minima, two of them corresponding to two herringbone configurations on the centered rectangular lattice with different dihedral angles, and the third one corresponding to a parallel configuration on an oblique lattice. The molecule geometrical parameter turns out to discriminate the lowest energy configuration. In Sec. IV a finite temperature analysis is carried out by minimizing a variational mean field free energy evaluated for molecules constrained to lie on a Bravais lattice. The optimization is carried out with respect to lattice parameters and to the orientational probability distributions. The model is studied upon varying temperature and the results of this investigation, namely, the temperature–surface-pressure phase diagram, unit cell parameters, and orientational probability densities, are then presented and discussed in Sec. V. Finally Sec. VI is devoted to some concluding remarks.

II. THE MODEL

The basic objects of our model are planar molecules, made up of four interaction centers, or ''atoms,'' placed on the vertices of a rectangle, as shown in Fig. 1. We shall assume that each atom of a molecule interacts with the atoms of all other molecules by means of a Lennard-Jones potential

$$V(r)=\frac{1}{r^{12}}-\frac{2}{r^{6}}, \tag{2.1}$$

where r is the distance between interaction centers. Let us note that Eq. (2.1) has been normalized in such a way that both depth and distance of the potential energy minimum turn out to be equal to 1, thus defining length and energy units. The circles in Fig. 1 have a conventional radius equal to half the distance of the potential minimum (1/2 with our normalization). For calculations we shall actually cut off $V(r)$ at some distance r_0, and use as a potential energy $\overline{V}(r)$, defined as follows:

$$\overline{V}(r)=V(r)-V(r_0), \quad r\leqslant r_0,$$

$$\overline{V}(r)=0, \quad r>r_0. \tag{2.2}$$

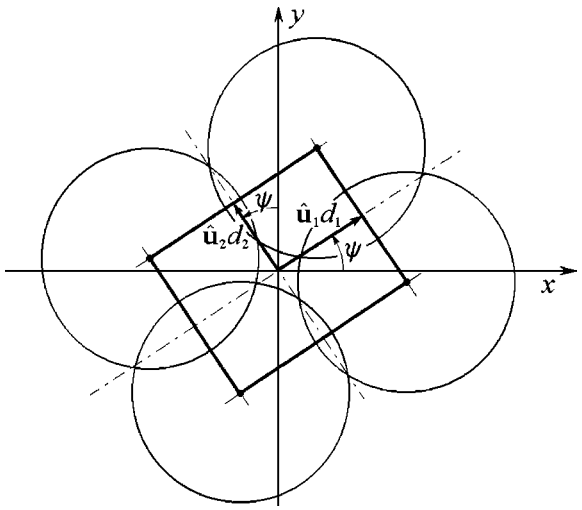

FIG. 1. Model molecule and its degrees of freedom. Vertices of the rectangle are interaction centers (circles represent hard cores); d_1 and d_2 are shape parameters. The degree of freedom is the angle ψ, denoting a (counterclockwise) rotation in the x,y plane. Unit vectors $\hat{\mathbf{u}}_1$ and $\hat{\mathbf{u}}_2$ define a frame of reference attached to the molecule.

The particular shape chosen for the model molecules can be motivated by the fact that, in a conformationally ordered (all *trans*) alkyl chain, hydrogen atoms are placed in pairs alternately on two opposite sides with respect to carbon atoms. Hence, on projecting the chain in a plane orthogonal to its axis, the positions of hydrogen atoms qualitatively correspond to the interaction centers of the model molecule. One can object that this model is extremely rough, because, besides the hypothesis of conformational order, the contribution of carbon atoms is completely neglected and hydrogen atoms are ''squeezed'' on a single plane. Nevertheless, we believe that two main features are needed to make herringbone packing possible: rotational symmetry breaking of molecules and the existence of small lateral ''cavities,'' according to the picture provided by close packing theory. Both these characteristics are present in our planar model molecules.

Assuming now that molecules can move freely (translate and rotate) in a plane, we calculate the interaction energy between two of them as a function of their (relative) position and their orientations with respect to a fixed axis, which we identify with the x axis. We can see (Fig. 1) that the positions of the vertices of the rectangle (with respect to the origin of axes) can be written in vector form as

$$\underline{d} = s_1 d_1 \hat{u}_1 + s_2 d_2 \hat{u}_2, \quad s_1, s_2 = \pm 1, \tag{2.3}$$

where d_1 and d_2 are geometrical parameters (half sides of the rectangle) and unit vectors $\hat{u}_1$ and $\hat{u}_2$ define a frame of reference attached to the molecule. Expressing $\hat{u}_1, \hat{u}_2$ as a function of unit vectors $\hat{x}, \hat{y}$ defining the fixed frame, and of the angle ψ, we can also write

$$\begin{aligned} \underline{d} &= (s_1 d_1 \cos\psi - s_2 d_2 \sin\psi)\hat{x} + (s_1 d_1 \sin\psi + s_2 d_2 \cos\psi)\hat{y} \\ &\doteq \underline{d}_{s_1 s_2}(\psi), \quad s_1, s_2 = \pm 1, \end{aligned} \tag{2.4}$$

where the dependence on the characteristic lengths d_1 and d_2 is not explicitly denoted. The interaction energy E of two molecules, whose centers are placed at certain positions represented by vectors $\underline{r}, \underline{r}'$, and whose orientations are respectively ψ, ψ', can be easily calculated by summing all interactions between pairs of ''atoms'' in opposite molecules, i.e.,

$$\begin{aligned} E &= \sum_{s_1, s_2, s_1', s_2'} \overline{V}(|\underline{r}' - \underline{r} + \underline{d}_{s_1' s_2'}(\psi') - \underline{d}_{s_1 s_2}(\psi)|) \\ &\doteq E(\underline{r}' - \underline{r}; \psi, \psi'), \end{aligned} \tag{2.5}$$

where summations are understood to run over $s_1, s_2, s_1', s_2' = \pm 1$. As a direct consequence of molecule symmetries, the pair interaction energy has the following properties: it is invariant under exchange of positions and orientations of the two interacting molecules,

$$E(-\underline{r}; \psi, \psi') = E(\underline{r}; \psi, \psi'), \tag{2.6}$$

$$E(\underline{r}; \psi', \psi) = E(\underline{r}; \psi, \psi'), \tag{2.7}$$

whereas a change of sign in both orientations turns out to be equivalent to a mirror symmetry with respect to the x or y axis,

$$E(\underline{r}; -\psi, -\psi') = E((\hat{x}\hat{x} - \hat{y}\hat{y}) \cdot \underline{r}; \psi, \psi') \tag{2.8}$$

$$= E((-\hat{x}\hat{x} + \hat{y}\hat{y}) \cdot \underline{r}; \psi, \psi') \tag{2.9}$$

[notice that Eq. (2.9) can be derived by Eq. (2.8) and (2.6)]. Equations (2.6), (2.7), (2.8), and (2.9) will be used later in order to simplify calculations.

Considering many interacting molecules the total interaction energy U can be simply written as the sum of pair interaction energies in the following way:

$$U = \frac{1}{2} \sum_{m,m'} \overline{\delta}_{mm'} E(\underline{r}_{m'} - \underline{r}_m; \psi_m, \psi_{m'}), \tag{2.10}$$

where m, m' label molecules, $\delta_{mm'}$ is a Kronecker delta, and the overbar denotes a Boolean inversion ($\overline{1} = 0$ and $\overline{0} = 1$); $\underline{r}_m$ and ψ_m ($\underline{r}_{m'}$ and $\psi_{m'}$) denote the position and orientation of molecule m (m').

III. GROUND STATE ANALYSIS

In this section we shall perform a ground state analysis but, in order to do so, we shall introduce two important simplifying hypotheses, supported by experimental observations and justified by analytical arguments (see the Appendix for details). The two hypotheses reduce the energy minimization to a tractable problem with a few variational parameters and consequently they do not consider the most general case, but it is possible to prove (Appendix) that the solutions found in this way are actually (local) minima of the total energy, with respect to *all* its independent variables (namely, molecule positions and orientations). Let us now introduce and discuss the two assumptions.

First of all we shall assume that *molecule centers are placed on the sites of a generic two-dimensional Bravais*

lattice (condition I). Notice, by the way, that this is a slightly more general case than the centered rectangular (distorted hexagonal) lattice, the common lattice structure of low temperature Langmuir monolayer condensed phases. Condition I can be written in the following way:

$$\underline{r}_m = \underline{R}_{(m_1,m_2)} \doteq m_1 \underline{a}_1 + m_2 \underline{a}_2 , \tag{3.1}$$

where the molecule label m is now understood as a two-dimensional index $m \doteq (m_1, m_2)$ running over all integer pairs, $\underline{a}_1, \underline{a}_2$ are basis vectors, and $\underline{R}_{(m_1,m_2)}$ is the generic vector of the Bravais lattice.

From a purely geometric point of view the lattice can be split into four (Bravais) sublattices, defined, respectively, by the parity of the two indices m_1, m_2. There are just four possibilities for (m_1, m_2), namely, (even,even), (even,odd), (odd,even), or (odd,odd). We shall assume that *all molecules in a sublattice have the same orientation* (condition II). In order to display parity explicitly, from now on we shall modify molecule (or site) labels into $m \doteq \gamma + n$, where $\gamma = (0,0),(0,1),(1,0),(1,1)$ is a parity index and $n = (n_1, n_2)$ another two-dimensional index where n_1, n_2 are any even integers. Condition II can then be written as

$$\psi_{\gamma+n} = \Psi_\gamma . \tag{3.2}$$

This hypothesis will be relaxed, at finite temperature, assuming that molecules in a sublattice have not the same orientations but only the same orientational probability density.

It is possible to show (see the Appendix) that the partial derivatives $\partial U / \partial \underline{r}_m$ of the total energy with respect to the position of each molecule, evaluated in the conditions I and II [Eqs. (3.1) and (3.2)], turn out to be zero. This is not yet sufficient to guarantee that a stationary point of the total energy is reached and an additional condition over orientations is needed. Nevertheless, this condition will be automatically supplied by the minimization with respect to sublattice orientations Ψ_γ, as discussed below.

Introducing assumptions (3.1) and (3.2) in the total energy expression (2.10), which we now rewrite in the new notation

$$U = \frac{1}{2} \sum_{\gamma,\gamma'} \sum_{n,n'} \overline{\delta_{\gamma\gamma'} \delta_{nn'}} E(\underline{r}_{\gamma'+n'} - \underline{r}_{\gamma+n}; \psi_{\gamma+n}, \psi_{\gamma'+n'}) \tag{3.3}$$

[where γ and γ' can take the values $(0,0),(0,1),(1,0),(1,1)$, whereas n and n' run over all pairs of even integers], we can write

$$U|_{\underline{R}\Psi} = \frac{1}{2} \sum_{\gamma,\gamma'} \sum_{n,n'} \overline{\delta_{\gamma\gamma'} \delta_{nn'}} E(\underline{R}_{\gamma'-\gamma+n'-n}; \Psi_\gamma, \Psi_{\gamma'}), \tag{3.4}$$

where the subscripts $\cdot|_{\underline{R}\Psi}$ denote just that the two conditions (3.1) and (3.2) have been applied. Moreover, the translational invariance of Bravais lattices allows us to write the inner sum (that over n') in the following way:

$$\sum_{n'} \overline{\delta_{\gamma\gamma'} \delta_{nn'}} E(\underline{R}_{\gamma'-\gamma+n'-n}; \Psi_\gamma, \Psi_{\gamma'}) \doteq v_{\gamma\gamma'}(\Psi_\gamma, \Psi_{\gamma'}), \tag{3.5}$$

which denotes explicitly that it is independent of n. Consequently, we can write

$$\sum_{n,n'} \overline{\delta_{\gamma\gamma'} \delta_{nn'}} E(\underline{R}_{\gamma'-\gamma+n'-n}; \Psi_\gamma, \Psi_{\gamma'}) = \frac{N}{4} v_{\gamma\gamma'}(\Psi_\gamma, \Psi_{\gamma'}), \tag{3.6}$$

where N is the total number of lattice sites, and hence

$$U|_{\underline{R}\Psi} = \frac{N}{8} \sum_{\gamma,\gamma'} v_{\gamma\gamma'}(\Psi_\gamma, \Psi_{\gamma'}). \tag{3.7}$$

The ground state energy, which we shall now denote by $U|_{\underline{R}\Psi}$, turns out to be a function only of the lattice basis vectors $\underline{a}_1$ and $\underline{a}_2$ and of the four angles Ψ_γ [$\gamma = (0,0),(0,1),(1,0),(1,1)$], each one representing a whole sublattice. It is possible to show (see the Appendix again) that if the derivatives of $U|_{\underline{R}\Psi}$ with respect to the sublattice angles $\partial U|_{\underline{R}\Psi} / \partial \Psi_\gamma$ vanish, then $\partial U / \partial \psi_m$, evaluated in the two conditions (3.1) and (3.2) also vanish $\forall m$. This ensures that a minimization of $U|_{\underline{R}\Psi}$, which we are going to perform in the following, provides also a stationary point of the total energy U with respect to all positions and orientations. A straightforward way to verify whether this is actually a minimum is discussed in the Appendix.

Before going on with the ground state analysis let us now introduce some symmetry properties of the previously defined functions $v_{\gamma\gamma'}(\Psi, \Psi')$, which will allow us to simplify analytical and numerical calculations both here and in the finite temperature analysis, which will be carried out in the next section. These properties come from the translation invariance of the Bravais lattice and from the symmetries of the pair interacion energy E, defined by Eqs. (2.7), (2.8), and (2.9). First of all, using the translation invariance of Eq. (3.5), we can show that $v_{\gamma\gamma'}$ does not depend on both indices γ, γ' but only on $(\gamma' - \gamma)_2$, that is,

$$v_{\gamma\gamma'}(\Psi, \Psi') = v_{(0,0)(\gamma'-\gamma)_2}(\Psi, \Psi'), \tag{3.8}$$

where $(\cdot)_2$ denotes that the argument in parentheses is to be considered modulo 2. This fact allows us to compute only four out of 16 functions of two angular variables. Moreover, Eq. (2.7), together with Eq. (3.5), allows us to show that

$$v_{\gamma\gamma'}(\Psi', \Psi) = v_{\gamma\gamma'}(\Psi, \Psi'), \tag{3.9}$$

whereas, due to Eqs. (2.8) and (2.9) it can easily be proved that, in the particular case of the rectangular lattice,

$$v_{\gamma\gamma'}(-\Psi, -\Psi') = v_{\gamma\gamma'}(\Psi, \Psi'). \tag{3.10}$$

In view of the ground state analysis we now have to minimize the energy (3.7) with respect to the angles Ψ_γ and the lattice basis vectors $\underline{a}_1$ and $\underline{a}_2$ (actually we shall consider the direction of $\underline{a}_1$ fixed along the x axis, so that $\underline{a}_1 = b\hat{x}$ and $2\underline{a}_2 = c\hat{x} + a\hat{y}$, as shown in Fig. 2, where a, b, c are scalar variational parameters). We perform a numerical minimum search, making use of standard optimization routines (MATLAB), using a large number of guess solutions, chosen to cover as uniformly as possible the set of allowed values of the variational parameters [as far as angular parameters are concerned the set can be conveniently reduced using the

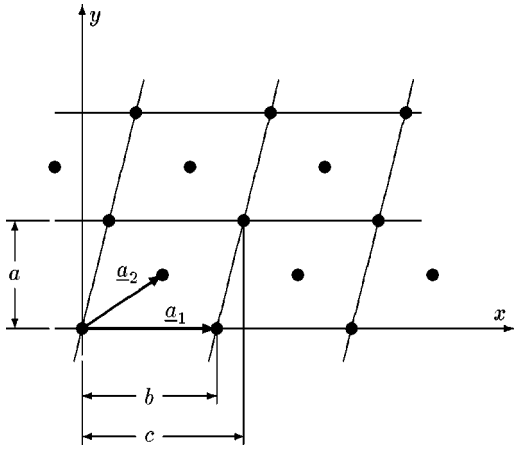

FIG. 2. Two-dimensional Bravais lattice and a possible choice of basis vectors $(\underline{a}_1,\underline{a}_2)$. Solid circles denote sites and thin solid lines denote two-site unit cells. Cell parameters are a,b,c. If $b=c$ a centered rectangular lattice is obtained.

symmetry property (3.9)]. We choose a cutoff distance $r_0=10$, which gives substantially correct results and avoids excessive computational effort, and the molecule geometrical parameters

$$1/d_1=3, \quad d_2/d_1\in[0,1], \tag{3.11}$$

representing a significant case in the framework of our model. Remembering that the length unit is the distance of the Lennard-Jones potential minimum, we notice that the choice of d_1 is in quite good agreement with alkyl chain parameters commonly used in the literature [14], whereas the values of the parameter d_2/d_1, which will be referred to as the *aspect ratio* from now on, can also move away from literature values. This is not so worrying because precise values of this parameter are not extremely meaningful in such a simplified model. As a result we obtain only three different minima, corresponding to states of the system sketched in Fig. 3 for the particular case $d_2/d_1=0.16$. In two of them molecules are packed on a centered rectangular lattice and display only two possible orientations, opposite with respect to the sides of the (centered) rectangular unit cell. With the choice of basis vectors displayed in Fig. 2 we have

$$\Psi_{(0,0)}=\Psi_{(1,0)}=-\Psi_{(0,1)}=-\Psi_{(1,1)}, \tag{3.12}$$

that is, only two sublattices can be distinguished. Opposite orientations characterize two different kinds of herringbone ordering, the former with higher angles (about 118° between backbone planes), the latter with lower angles (about 35° between backbone planes). They can be naturally related to HB and PHB packing modes, even if the angle values do not coincide with those predicted by more detailed models [13,14]. The numerical values of the lattice parameters (a and $b=c$) are also reported to allow a comparison with experimentally observed lattice distortions. Precise values are not quantitatively correct but we realize that the HB minimum corresponds to a nearest neighbor distortion ($b<a\sqrt{3}$) and the PHB minimum to a next nearest neighbor distortion ($b>a\sqrt{3}$), according to experimental results. In the third minimum the lattice becomes oblique and molecules display equal orientations on the whole lattice, that is,

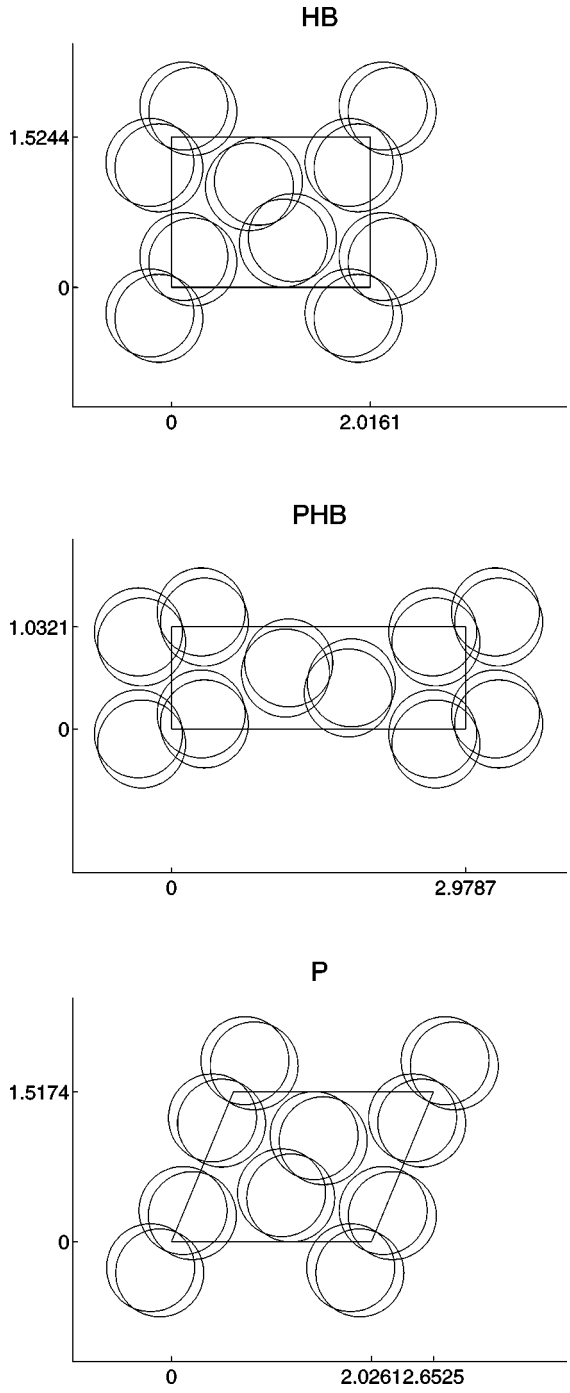

FIG. 3. Herringbone (HB), pseudoherringbone (PHB), and parallel (P) packing modes, corresponding to the ground state energy minima in the case $1/d_1=3.0$ and $d_2/d_1=0.16$. On the axes one can read the lattice parameters corresponding to a nearest neighbor distortion in the HB case, a next nearest neighbor distortion in the PHB case, and an intermediate distortion for the P case.

$$\Psi_{(0,0)}=\Psi_{(1,0)}=\Psi_{(0,1)}=\Psi_{(1,1)}. \tag{3.13}$$

As already mentioned in the Introduction, this kind of configuration, which from now on will be referred to as *parallel* (P), is rarely observed in Langmuir monolayers, except for the case of chiral resolved amphiphiles, in which our results about lattice distortions again qualitatively agree with those obtained in experiments (see, for instance, Ref. [15]). Actu-

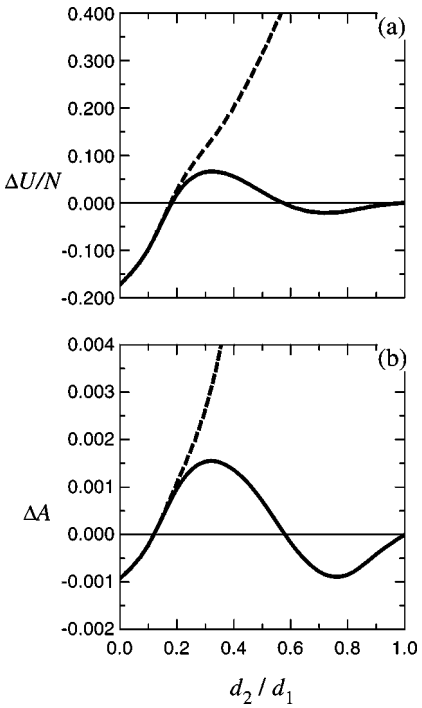

FIG. 4. Energy (a) and area per molecule (b) differences between P and HB phases (solid lines), and between PHB and HB phases (dashed lines), plotted vs molecule aspect ratio d_2/d_1.

ally our model does contain a single type of molecule because there is nothing in the model potential that can distinguish molecules of different chirality. All these results are quite interesting because they prove that the model, in spite of drastic simplifying assumptions, can actually predict different kinds of orientational ordering (herringbone, pseudoherringbone, parallel) and also the corresponding lattice distortions in a qualitatively correct way.

Taking into account values of energy and area per molecule for the different packing modes, we realize that the aspect ratio d_2/d_1 is relevant to discriminate between the modes. In Figs. 4(a) and 4(b) we report the differences between the PHB and HB and between the P and HB minima, in terms of energy and area per molecule, respectively, as functions of d_2/d_1. It turns out [see Fig. 4(a)] that for low values of the aspect ratio (less than about 0.18) the PHB and P packing modes are energetically favored and nearly degenerate, with a slight predominance for the P packing; for higher values of d_2/d_1 (up to about 0.58) the HB minimum takes on a lower energy; and finally, for still higher values (up to 1), the P packing is again favored. The lowest energy phase is the stable one at zero (or low) surface pressure. On the contrary, if the effect of pressure has to be taken into account, the stable phase is determined by the lowest enthalpy ($U/N+\Pi A$, Π being the surface pressure itself, and $A=ab/2$ the area per molecule). In the high pressure limit the pressure-area (ΠA) term becomes dominating and the stable phase is simply determined as that with the lowest area per molecule, which should be determined in principle by repeating the above described variational procedure but searching for minima of the enthalpy, which we have actually performed. Nevertheless, it has turned out that the system behavior is well predicted (from a qualitative point of view) simply by the zero pressure value of the area per molecule, reported in Fig. 4(b). Generally the lowest energy phase (at zero pressure) is also the one with the lowest area per molecule, that is, the predominant phase at zero pressure is predominant at infinite pressure as well. A different behavior is observed only for a range of values of the aspect ratio around $d_2/d_1=0.16$, in which the P packing mode (nearly degenerate with PHB) has the lowest energy but a slightly larger area per molecule than the HB mode. This fact gives rise to a phase transition between P and HB at $\Pi\approx 53$, as will be pointed out more clearly in Sec. V, where the temperature–surface-pressure phase diagram is presented.

IV. MEAN FIELD THEORY

In this section we shall perform a finite temperature analysis of the model by means of a mean field approximation. We shall write an approximated Gibbs free energy for a system of molecules constrained to lie on a generic two-dimensional Bravais lattice and assumed to have only four possible orientational probability distributions, depending on the sublattice, as mentioned in the previous section. The free energy is then a function of lattice parameters (a,b,c) and probability densities on the four sublattices, which will be used as variational parameters. Let us note that only orientations are assumed to be random variables and hence only the orientational entropy contribution is taken into account.

The internal energy can be written as

$$\mathcal{U}=\langle U|_{\underline{R}}\rangle_{\Psi} =\frac{1}{2}\sum_{\gamma,\gamma'}\sum_{n,n'}\overline{\delta_{\gamma\gamma'}\delta_{nn'}}\langle E(\underline{R}_{\gamma'-\gamma+n'-n};\psi_{\gamma+n},\psi_{\gamma'+n'})\rangle, \tag{4.1}$$

where the energy $U|_{\underline{R}}$ is given by Eq. (3.3) in the condition (3.1), which is denoted by the subscript $\cdot|_{\underline{R}}$, and $\langle\cdot\rangle_{\Psi}$ denotes a thermal average over orientation variables. As mentioned above, we assume that the probability density of a molecule orientation at site $\gamma+n$, which we may denote by $f_{\gamma+n}(\psi)$, actually depends on the sublattice only, i.e.,

$$f_{\gamma+n}(\cdot)=F_{\gamma}(\cdot), \quad \forall\,\gamma,n. \tag{4.2}$$

Assuming that molecule orientations at different sites are statistically independent variables (mean field approximation), the pair probability density can be factorized to give

$$\mathcal{U}=\frac{1}{2}\sum_{\gamma,\gamma'}\sum_{n,n'}\overline{\delta_{\gamma\gamma'}\delta_{nn'}}\int_{-\pi/2}^{\pi/2}d\Psi F_{\gamma}(\Psi) \times\int_{-\pi/2}^{\pi/2}d\Psi' F_{\gamma'}(\Psi')E(\underline{R}_{\gamma'-\gamma+n'-n};\Psi,\Psi'), \tag{4.3}$$

where, because of the twofold symmetry of the model molecules, integrals can be evaluated over $[-\pi/2,\pi/2]$ (instead of $[-\pi,\pi]$). Probability densities must be normalized over $[-\pi/2,\pi/2]$, too. Making use of Eq. (3.6) with $\Psi_{\gamma}=\Psi$ and $\Psi_{\gamma'}=\Psi'$, we obtain

$$\mathcal{U}=\frac{N}{8}\sum_{\gamma,\gamma'}\int_{-\pi/2}^{\pi/2}d\Psi F_\gamma(\Psi)\int_{-\pi/2}^{\pi/2}d\Psi' F_{\gamma'}(\Psi') \times v_{\gamma\gamma'}(\Psi,\Psi'). \tag{4.4}$$

As far as the entropy is concerned, the mean field approximation gives

$$\mathcal{S}=-\frac{Nk_B}{4}\sum_{\gamma}\int_{-\pi/2}^{\pi/2}d\Psi F_\gamma(\Psi)\ln F_\gamma(\Psi), \tag{4.5}$$

where k_B is the Boltzmann constant and an additive constant has been neglected.

The Gibbs free energy functional is

$$\mathcal{G}=\mathcal{U}+N\Pi A-T\mathcal{S}-\frac{N}{4}\sum_{\gamma}\lambda_\gamma\left(\int_{-\pi/2}^{\pi/2}d\Psi F_\gamma(\Psi)-1\right), \tag{4.6}$$

where $\mathcal{U}$ and $\mathcal{S}$ are internal energy and entropy, respectively, defined by Eqs. (4.4) and (4.5), T is the absolute temperature, Π the surface pressure, and $A=ab/2$ the area per molecule. The last term, containing four unknown Lagrange multipliers λ_γ, is needed to ensure normalization of probability densities and multipliers must be determined by imposing normalization constraints. The free energy functional must be minimized with respect to probability densities and unit cell parameters. Its first variation with respect to these quantities can be written as

$$\delta\mathcal{G}=\sum_{\gamma}\int_{-\pi/2}^{\pi/2}d\Psi\frac{\delta\mathcal{G}}{\delta F_\gamma(\Psi)}\delta F_\gamma(\Psi)+\sum_{\xi=a,b,c}\frac{\partial\mathcal{G}}{\partial\xi}\delta\xi \tag{4.7}$$

where $\delta\mathcal{G}/\delta F_\gamma(\Psi)$ denotes a functional derivative.

Making use of the symmetry properties (3.8) and (3.9), we have

$$\frac{\delta\mathcal{G}}{\delta F_\gamma(\Psi)}=\frac{N}{4}\sum_{\gamma'}\int_{-\pi/2}^{\pi/2}d\Psi' F_{\gamma'}(\Psi')v_{\gamma\gamma'}(\Psi,\Psi') +\frac{N}{4}k_BT[\ln F_\gamma(\Psi)+1]-\frac{N}{4}\lambda_\gamma. \tag{4.8}$$

Moreover, as far as derivatives with respect to lattice parameters are concerned, we have

$$\frac{\partial\mathcal{G}}{\partial\xi}=\frac{N}{4}\sum_{\gamma,\gamma'}\int_{-\pi/2}^{\pi/2}d\Psi F_\gamma(\Psi)\int_{-\pi/2}^{\pi/2}d\Psi' F_{\gamma'}(\Psi') \times\frac{\partial v_{\gamma\gamma'}(\Psi,\Psi')}{\partial\xi}+N\Pi\frac{\partial A}{\partial\xi}, \tag{4.9}$$

where $\xi=a,b,c$ and

$$\frac{\partial A}{\partial a}=\frac{b}{2},\quad \frac{\partial A}{\partial b}=\frac{a}{2},\quad \frac{\partial A}{\partial c}=0, \tag{4.10}$$

whereas $\partial v_{\gamma\gamma'}(\Psi,\Psi')/\partial\xi$ can be evaluated from Eqs. (3.5), (2.5), and (2.1).

In order to find the stationary points (actually the minima) of the free energy functional we set to zero the derivatives (4.8) and (4.9). After some manipulation the first condition can be written as

$$F_\gamma(\Psi)=\frac{\exp\left(-\sum_{\gamma'}\int_{-\pi/2}^{\pi/2}d\Psi' F_{\gamma'}(\Psi')\beta v_{\gamma\gamma'}(\Psi,\Psi')\right)}{\exp(1-\beta\lambda_\gamma)}, \tag{4.11}$$

where $\beta=1/k_BT$ and, for normalization,

$$\exp(1-\beta\lambda_\gamma)=\int_{-\pi/2}^{\pi/2}d\Psi\exp\left(-\sum_{\gamma'}\int_{-\pi/2}^{\pi/2}d\Psi' F_{\gamma'}(\Psi') \times\beta v_{\gamma\gamma'}(\Psi,\Psi')\right). \tag{4.12}$$

This form naturally suggests an iterative numerical solution, in which the right-hand side is the current iteration step and the left-hand side represents the next one. Also, the equations obtained by setting to zero Eq. (4.9) can be put in a fixed point form. Among different possible forms we have chosen the following one:

$$\xi=\xi\exp\left(-\alpha\frac{\partial\mathcal{G}/N}{\partial\xi}\right), \tag{4.13}$$

where α is a relaxation parameter, needed to stabilize the procedure. Equations (4.11) and (4.13) are coupled with each other and hence they are to be solved by a single procedure, which we have implemented in the following way.

(1) A guess solution is defined in terms of probability densities $F_\gamma(\Psi)$ and unit cell parameters a,b,c.

(2) Functions $v_{\gamma\gamma'}(\Psi,\Psi')$ are evaluated for the assigned values of a,b,c and the iterative procedure defined by Eq. (4.11) is carried out, approximating integrals by means of common Gaussian quadrature formulas, until convergence is reached for the probability densities.

(3) A new estimate of a,b,c is computed using Eq. (4.13) with the probability densities evaluated at the previous step (a reasonable choice of the relaxation parameter has turned out to be $\alpha\approx10^{-3}$).

(4) Steps 2 and 3 are repeated until convergence is reached for both probability densities and lattice parameters.

Using different guess solutions the above iterative procedure allows us to determine local minima of the Gibbs free energy and the stable phase is determined as that corresponding to the absolute minimum. Guess solutions are chosen in the following way: probability densities with peaks centered around certain angle values (among which are those corresponding to ground state HB, PHB, and P packing modes) for ordered phases and a uniform density over the whole range $[-\pi/2,\pi/2]$ for the orientationally disordered phase.

V. FINITE TEMPERATURE BEHAVIOR

In this section we shall describe the phase diagram in some detail and we shall characterize each phase in terms of angular probability densities and lattice parameters. As far as molecule geometric parameters are concerned, we have cho-

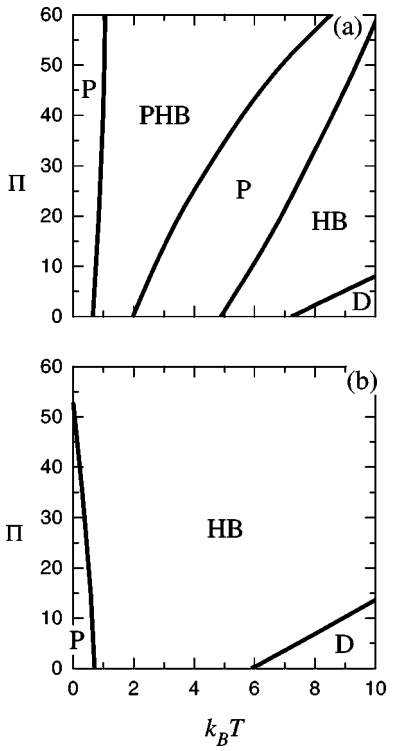

FIG. 5. Phase diagram in the temperature–surface-pressure plane for the two values of the aspect ratio $d_2/d_1=0$ (a) and $d_2/d_1=0.16$ (b) (in both cases $1/d_1=3.0$). HB, PHB, and P denote stability regions for herringbone, pseudoherringbone, and parallel phases, respectively; D is the disordered phase. Solid lines denote first order transitions.

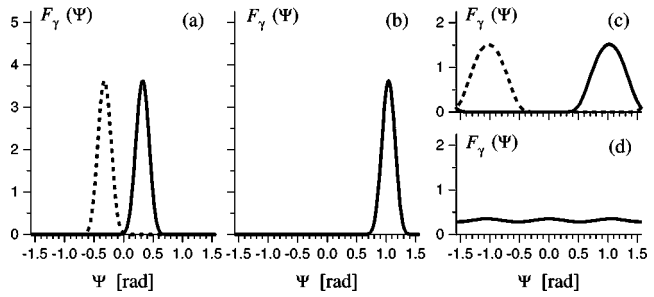

FIG. 6. Angular probability densities $F_{(0,0)}(\Psi)=F_{(1,0)}(\Psi)$ (solid lines) and $F_{(0,1)}(\Psi)=F_{(1,1)}(\Psi)$ (dashed lines) near two phase transitions in the two cases $d_2/d_1=0,0.16$, respectively, $(1/d_1=3.0)$: (a) $k_BT=4.5$, $\Pi=30.0$, $d_2=0$ (PHB phase); (b) $k_BT=4.5$, $\Pi=30.0$, $d_2=0$ (P phase); (c) $k_BT=8.0$, $\Pi=6.9$, $d_2/d_1=0.16$ (HB phase); (d) $k_BT=8.0$, $\Pi=6.8$, $d_2/d_1=0.16$ (disordered phase). In (b) and (d) one has $F_{(0,0)}(\Psi)=F_{(1,0)}(\Psi)=F_{(0,1)}(\Psi)=F_{(1,1)}(\Psi)$ (solid line).

sen $1/d_1=3.0$, as in ground state calculations, analyzing in detail the two significant cases $d_2/d_1=0,0.16$, which will be simply referred to as cases (a) and (b) in the following. In Figs. 5(a) and 5(b) the respective temperature–surface-pressure phase diagrams are reported. Let us consider the low pressure region first. In both cases it turns out that for some temperature [$k_BT\approx4.9$ in case (a) and $k_BT\approx0.7$ in case (b)] the P phase, which is stable in the ground state, becomes metastable, because the HB phase takes on a lower free energy value, and the phase transition is first order. At a higher temperature [$k_BT\approx7.2$ for (a) and $k_BT\approx5.9$ for (b)] the transition to an orientationally disordered phase, again first order, takes place. Case (a) is significantly different because a large (reentrant) stability region of the PHB phase is observed in the P phase region, probably due to the fact that the energy and area per molecule of these two packing modes are nearly equal for low values of the aspect ratio. A similar behavior can be observed actually for d_2/d_1 up to about 0.05. Cases (a) and (b) turn out to be significantly different upon increasing surface pressure, too. As far as the order-disorder transition is concerned a simple (nearly linear) increase of transition temperature is observed, which can be easily explained in the following way. Considering that the disordered phase, which must have a higher entropy, has also a higher area per molecule, the transition pressure must increase with temperature, according to the Clausius-Clapeyron equation. On the contrary, the transition between the ordered (P and HB) phases undergoes drastic changes depending on the aspect ratio d_2/d_1, because the area per molecule required by the two packing modes strongly depends on this geometric parameter. Two different behaviors can be observed, namely, in case (a) the transition temperature increases with increasing pressure, pointing out that HB packing is less dense than P, whereas in case (b) the transition temperature decreases, due to the fact that HB packing is denser. In the latter case the transition temperature vanishes at some pressure ($\Pi\approx53$), according to ground state results. Moreover, the two transitions that delimit the PHB phase region in case (a) display two different behaviors, namely, the lower temperature one is nearly vertical (meaning a nearly equal packing density of P and PHB phases), whereas the higher temperature one has a positive slope which increases with increasing pressure (meaning that the high temperature/high pressure P phase has a far lower packing density). Let us note finally that, if the aspect ratio is further increased (for instance, up to $d_2/d_1=0.2$), the P (and PHB) phase regions completely disappear, that is, these two packing modes are no longer convenient. Only one first order transition to the disordered phase takes place and the transition temperature is considerably lower than in previous cases (for instance, $k_BT=2.84$ at $\Pi=0$ for the case $d_2/d_1=0.4$). For still higher values of the aspect ratio the P phase becomes stable again and even in this case it is the only ordered stable phase, with a still lower transition temperature to the D phase (for instance, $k_BT=1.66$ at $\Pi=0$ for the case $d_2/d_1=0.8$).

In order to provide a more complete description of the system behavior we now also report angular probability densities for the different phases (Fig. 6), for some temperature and surface pressure values in the vicinity of significant transitions in cases (a) and (b). We can observe that, near the PHB-P transition of case (a), probability densities are centered around mean values very close to ground state angles, and quite strong peaks show that the system is still in a low temperature regime. Peak heights (and hence standard deviations) are almost the same for the two coexisting phases. Here herringbone ordering can be recognized by the fact that sublattice probability densities $F_{(0,0)}(\Psi)=F_{(1,0)}(\Psi)$ and $F_{(0,1)}(\Psi)=F_{(1,1)}(\Psi)$ break the symmetry $\Psi\rightarrow-\Psi$, whereas $F_{(\gamma_1,0)}(\Psi)=F_{(\gamma_1,1)}(-\Psi)$. On the contrary, parallel ordering is characterized by $F_{(0,0)}(\Psi)=F_{(1,0)}(\Psi)$

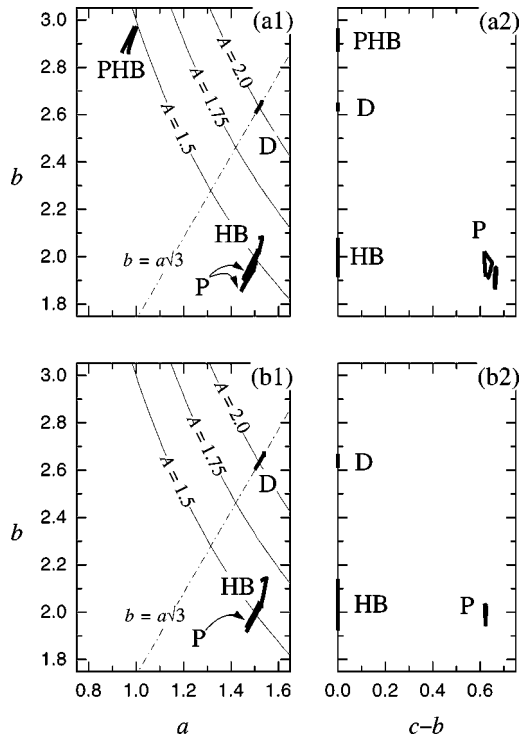

FIG. 7. Unit cell parameters (a,b,c) corresponding to the phase diagrams displayed in Fig. 5: $d_2=0$ (a1,a2) and $d_2/d_1=0.16$ (b1,b2), with $1/d_1=3.0$ in both cases. In (a1,b1) and (a2,b2) the projections onto the a,b and $(c-b),b$ planes are reported, respectively. Thick solid lines mark the boundaries of stability regions of each phase and the mapping of the $T=0$ and $\Pi=0$ lines, as far as the fictitious boundary $\Pi=60$, $k_BT=10$ (not illustrated). HB, PHB, P denote, respectively, herringbone, pseudoherringbone, parallel packing modes, and D is the disordered phase. Contour lines of the area per molecule $A=ab/2$ are also reported (thin solid lines) as well as the hexagonal unit cell condition (thin dash-dotted line).

$=F_{(0,1)}(\Psi)=F_{(1,1)}(\Psi)$. Moreover, at the transition between HB and disordered phases [in case (b)], we see that densities for the HB phase are broader, whereas in the disordered phase symmetry is restored and $F_{(\gamma_1,0)}(\Psi)=F_{(\gamma_1,1)}(\Psi)$.

It is interesting to inspect also lattice parameters obtained by finite temperature calculations, because they can be directly compared with experimental data. In Figs. 7(a1,a2) and 7(b1,b2) we report a mapping of the boundaries of the various phase regions displayed in Figs. 5(a) and 5(b), respectively, onto the lattice parameter planes a,b and $(c-b),b$. We can observe that ordered phases (HB and PHB) are placed on opposite sides of the line $b=a\sqrt{3}$ (which denotes an undistorted hexagonal lattice) and are characterized by nearest neighbor and next nearest neighbor distortions, respectively. In the a,b plane the P phase turns out to be completely superposed on HB and can be distinguished only in the $(c-b),b$ plane, revealing the oblique lattice. Increasing pressure drives lattice parameters toward lower area per molecule values, whereas a higher temperature corresponds to higher areas. On the contrary, the disordered phase regions are mapped exactly onto the line $b=a\sqrt{3}$ and only a pressure effect can be appreciated. In case (b) the system reaches higher area per molecule values, because molecules have a larger intrinsic area.

Let us now discuss model results in comparison with experiments, beginning from unit cell parameters. As previously mentioned, our two-dimensional model excludes tilt effects, projecting the monolayer in the plane orthogonal to the molecule long axes, and hence it is natural to take as a term of comparison experimentally measured projected parameters [13]. It turns out that calculated data well reproduce (qualitatively) experimental findings: the two opposite unit cell distortions, corresponding to HB and PHB packing modes, and also the transition to a rotationally disordered phase with a hexagonal (undistorted) unit cell are observed. Actually, the model predicts a clear discontinuity between lattice parameters of ordered and disordered phases, whereas this discontinuity does not seem to show in the experimental data of Ref. [13]. Nevertheless, it is known that the herringbone transition in Langmuir monolayers is weakly first order [7] and this may be a reason why the discontinuity does not emerge from measured parameters. Moreover, we note that the data reported in Ref. [13] come from the superposition of measurements performed on different substances, which might actually mask a weak discontinuity. Such a large quantity of measured parameters are not available for oblique lattice packings, which, however, have been observed in experiments as well. The comparison with experiments can be performed with respect to the temperature–surface-pressure phase diagram, too, and upon varying the molecule aspect ratio d_2/d_1. We state in advance that, if the transverse dimension (d_2) is not negligible, the structure of the model molecules should be more similar to real cross sections of alkyl chains [14] and hence the model should better reproduce a real system behavior. As we previously pointed out, the model predicts that for low values of the aspect ratio [case (a)] PHB and P packing modes turn out to be denser than HB. This is perhaps not the case in real systems, where, for instance, a PHB phase can sometimes be observed at lower surface pressure (L_{2h} phase for fatty acids) and a HB packing at higher pressure (CS, L_2'', S, and L_2' phases). Moreover, no experimental evidence has been obtained so far about the existence of three different packing modes for the same monolayer in different thermodynamic conditions. A different condition, more consistent with experiments, is reached, for instance, in case (b) $(d_2/d_1=0.16)$, where the PHB and P phases are less dense than the HB. A phase transition can be observed, in some temperature range, between a lower pressure P phase and a higher pressure HB phase, but the free energy of P is very similar to that of PHB, which might be easily stabilized by a small perturbation of the interaction energy, such as a chiral head group, giving rise to the experimentally observed low pressure PHB phase. Actually, the calculated temperature–surface-pressure phase diagram [Fig. 5(b)] would still display some qualitative difference with respect to the experimental one, even in this case. First of all the P- (PHB-) HB transition turns out to be mainly driven by temperature, whereas in experiments it seems to be mainly driven by pressure and coincides with the swiveling (L_{2h}-L_2') transition, and secondly the P (PHB) phase region is placed at low temperature, whereas in experiments a direct PHB-disordered transition (L_{2h}-L_{2d}) has been observed [30]. Possible reasons for discrepancies, especially in the low pressure regime, may be found in the simplified way in which the model takes into account effects of compression. The lattice can be strained but actually unit cell

parameters are not random variables and hence the only contribution to entropy is the orientational one. Moreover, tail effects, which should have some importance especially in the low pressure behavior of the system, are neglected by construction by the model, as well as the existence of vacancies (empty sites) in the lattice, which is not allowed. In this way the monolayer turns out to be scarcely compressible, and it can be verified that the area per molecule undergoes only some percentage variation for pressure varying by an order of magnitude. Another important issue is the stability of our ordered phases with respect to fluctuations that might destroy or weaken long range order. Since it is known [22–24] that the mean field approximation performs poorly in describing the herringbone transition in systems of molecules adsorbed on graphite (wrong order of the transition, overestimated transition temperature), it would be of great interest to investigate the present model using numerical simulations and/or more accurate semianalytic tools like the Bethe approximation and the cluster variation method, but this is beyond the scope of the present work.

VI. CONCLUSIONS

In this paper we have introduced a planar-molecule model to describe backbone plane ordering in amphiphilic monolayers. The main characteristics of the model are the molecule shape (which has been chosen to mimic the cross section of alkyl chains), Lennard-Jones interactions between ''atoms'' (interaction centers), and the introduction of a regular but deformable lattice, in order to analyze different (experimentally observed) unit cell distortions upon varying external thermodynamic variables. The molecules possess a twofold rotational symmetry, which is needed to reproduce herringbone ordering, and molecule orientations are described as continuous degrees of freedom. A ground state analysis was first performed, by minimizing the interaction energy with respect to molecule positions and backbone angles. It was shown that an energy minimum is reached if molecules are placed on a generic two-dimensional Bravais lattice with regularly modulated orientations, and that the minimum search problem can be reduced to an optimization with respect to a few variational parameters, namely, sublattice orientations and unit cell parameters. It has been pointed out that the model predicts three different kinds of orientational ordering, two of them known in the literature as herringbone and pseudoherringbone, displaying finite dihedral angles between differently oriented molecules, and the third one with all molecules aligned. The competition between the different minima has been investigated as a function of molecule aspect ratio, pointing out that a different packing mode may be favored by a different molecule geometry. Lattice distortions are found to be in good qualitative agreement with experimental observations. A finite temperature analysis has also been performed in the framework of a mean field approximation, maintaining the ground state lattice structure, but allowing lattice parameters to vary. The temperature evolution of each ordered (herringbone, pseudoherringbone, and parallel) phase has been analyzed, determining phase transitions between one another and a (first order) transition to the orientationally disordered phase, which displays an undistorted hexagonal unit cell. Some discrepancies of model predictions with respect to experimental findings (especially in the temperature behavior) have been found and discussed. In particular, the discontinuity in lattice parameters between ordered and disordered phases is not observed in experimental values, most likely because of a weak first order transition. Moreover, the competition between P and PHB phases is probably unresolved, because they have a very similar free energy in a significant range of values of the molecule aspect ratio, and hence small perturbations of the model potential might have important effects. In contrast, some differences in the transition between ordered [HB and P (PHB)] phases may be ascribed to the fact that only the orientational entropy contribution has been taken into account.

ACKNOWLEDGMENT

This work was supported by MURST through the research project ''Structure and Dynamics of Biologically Interesting Monolayers.''

APPENDIX

In this Appendix we shall prove rigorously that the states obtained by the minimization of the energy $U_{R\Psi}$ [Eq. (3.3)], performed with respect to the basis vectors $\underline{\underline{a}}_1, \underline{\underline{a}}_2$ of the Bravais lattice and to the sublattice orientations Ψ_γ as described in the text, are actually (local) minima of the total energy U [Eq. (2.10)], considered as a function of all positions $\underline{r}_m$ and orientations ψ_m of molecules m.

First of all we can see that the derivative (gradient) of the energy U with respect to the position of a molecule $\underline{r}_m$, evaluated in the hypothesis (3.1), that is, for molecules staying on a generic Bravais lattice (which is denoted by the symbol $\cdot|_{\underline{\underline{R}}}$), can be written as

$$\left.\frac{\partial U}{\partial \underline{r}_m}\right|_{\underline{\underline{R}}} = \frac{1}{2}\sum_{m'} \overline{\delta_{m'}}[\underline{\underline{E}}^{(r)}(\underline{R}_{m'};\psi_m,\psi_{m-m'}) - \underline{\underline{E}}^{(r)}(\underline{R}_{m'};\psi_m,\psi_{m+m'})]. \tag{A1}$$

To write Eq. (A1) we have employed the symmetry property (2.6) and the inversion symmetry of the Bravais lattice. We have also defined $\underline{\underline{E}}^{(r)}$ to be the derivative (gradient) of the pair interaction energy E [Eq. (2.5)] with respect to the positional argument, and $\delta_m = 1$ if $m = (0,0)$ and 0 otherwise. Equation (A1) tells us that a sufficient condition for the positional derivatives to vanish (provided molecules are placed on a Bravais lattice) is $\psi_{m+m'} = \psi_{m-m'} \ \forall m,m'$. Moreover, it is easy to see that this condition is equivalent to the fact that ψ_m depends only on the parity of the index m [we remember that it is actually a two-dimensional index $m = (m_1, m_2)$ and hence we have the four possibilities (even, even), (even,odd), (odd,even), (odd,odd)]. The lattice is split into four sublattices with double lattice constants, and molecules placed on the same sublattice must have the same orientation. As already performed in the text, we then introduce the new notation $m = \gamma + n$, where $\gamma = (0,0),(0,1),(1,0),(1,1)$ is the parity index and $n = (n_1, n_2)$ any pair of even integers. The above condition is thus expressed by Eq. (3.2).

We now write, in the new notation, the derivative of the energy with respect to a generic molecule orientation $\psi_{\gamma+n}$, evaluated with the assumptions on positions [Eq. (3.1)] and orientations [Eq. (3.2)] discussed above, which will be denoted as a whole by the double subscript $\cdot|_{\underline{\underline{R}}\Psi}$. Using the translation invariance of a Bravais lattice, we obtain

$$\left.\frac{\partial U}{\partial \psi_{\gamma+n}}\right|_{\underline{\underline{R}}\Psi} = \sum_{\gamma'} \sum_{n'} \overline{\delta_{\gamma\gamma'}\delta_{n'}} E^{(\psi_1)}(\underline{R}_{\gamma'-\gamma+n'}; \Psi_\gamma, \Psi_{\gamma'}), \tag{A2}$$

where $E^{(\psi_1)}$ is the derivative of E with respect to the former angular argument. We also rewrite Eq. (3.4), that is, the total energy under the same conditions, using again the translation invariance of the Bravais lattice. With N as the total number of lattice sites, we have

$$U_{\underline{\underline{R}}\Psi} = \frac{N}{8} \sum_{\gamma,\gamma'} \sum_{n'} \overline{\delta_{\gamma\gamma'}\delta_{n'}} E(\underline{R}_{\gamma'-\gamma+n'}; \Psi_\gamma, \Psi_{\gamma'}), \tag{A3}$$

which turns out to be a function only of the sublattice orientations Ψ_γ and of the basis vectors $\underline{a}_1, \underline{a}_2$. From Eqs. (A3) and (A2) it is possible to show that the following identity holds:

$$\frac{\partial}{\partial \Psi_\gamma} U_{\underline{\underline{R}}\Psi} = \frac{N}{4} \left.\frac{\partial U}{\partial \psi_{\gamma+n}}\right|_{\underline{\underline{R}}\Psi}. \tag{A4}$$

The left-hand side (the derivative of the conditioned energy with respect to sublattice orientations) is imposed to be zero by our numerical minimization procedure. This proves that the derivative with respect to a generic molecule orientation also vanishes, completing the first step of our proof. Let us only note that the two ingredients to prove Eq. (A4) are just the two conditions (3.1) and (3.2).

Let us now consider the Hessian matrix, that is, the second derivatives with respect to positions and orientations of any pair of molecules (indexed by m, m'), and the associated eigenvalue equation

$$\sum_{m'} \begin{bmatrix} \dfrac{\partial^2 U}{\partial \underline{r}_m \partial \underline{r}_{m'}} & \dfrac{\partial^2 U}{\partial \underline{r}_m \partial \psi_{m'}} \\ \dfrac{\partial^2 U}{\partial \psi_m \partial \underline{r}_{m'}} & \dfrac{\partial^2 U}{\partial \psi_m \partial \psi_{m'}} \end{bmatrix} \cdot \begin{bmatrix} \delta \underline{r}_{m'} \\ \delta \psi_{m'} \end{bmatrix} = \lambda \begin{bmatrix} \delta \underline{r}_m \\ \delta \psi_m \end{bmatrix}. \tag{A5}$$

Let us note that, considering a fixed pair of molecules, we have a 3×3 matrix (which is explicitly denoted by the square brackets) but every element of this matrix must have actually the two indices m, m', giving rise to an infinite matrix. This can also be regarded as composed of an infinite number ($N\times N$, N being the number of molecules) of 3×3 blocks. We have to prove that the states found by our minimization satisfy $\lambda > 0$. Imposing the usual conditions we can write (in the new notation)

$$\begin{aligned} &\begin{bmatrix} \dfrac{\partial^2 U}{\partial \underline{r}_{\gamma+n} \partial \underline{r}_{\gamma'+n'}} & \dfrac{\partial^2 U}{\partial \underline{r}_{\gamma+n} \partial \psi_{\gamma'+n'}} \\ \dfrac{\partial^2 U}{\partial \psi_{\gamma+n} \partial \underline{r}_{\gamma'+n'}} & \dfrac{\partial^2 U}{\partial \psi_{\gamma+n} \partial \psi_{\gamma'+n'}} \end{bmatrix}_{\underline{\underline{R}}\Psi} \\ &= \overline{\delta_{\gamma\gamma'}\delta_{n'-n}} \underline{\underline{\mathbf{E}}}_{12}(\underline{R}_{\gamma'-\gamma+n'-n}; \Psi_\gamma, \Psi_{\gamma'}) \\ &\quad + \delta_{\gamma\gamma'}\delta_{n'-n} \sum_{\gamma''} \sum_{n''} \overline{\delta_{\gamma\gamma''}\delta_{n''}} \\ &\quad \times \underline{\underline{\mathbf{E}}}_{11}(\underline{R}_{\gamma''-\gamma+n''}; \Psi_\gamma, \Psi_{\gamma''}) \\ &\doteq \underline{\underline{\mathbf{h}}}_{\gamma\gamma',n'-n}, \end{aligned} \tag{A6}$$

where

$$\underline{\underline{\mathbf{E}}}_{12} \doteq \begin{bmatrix} -\underline{\underline{E}}^{(rr)} & -\underline{E}^{(r\psi_2)} \\ \underline{E}^{(\psi_1 r)} & E^{(\psi_1\psi_2)} \end{bmatrix}, \tag{A7}$$

$$\underline{\underline{\mathbf{E}}}_{11} \doteq \begin{bmatrix} \underline{\underline{E}}^{(rr)} & -\underline{E}^{(r\psi_1)} \\ -\underline{E}^{(\psi_1 r)} & E^{(\psi_1\psi_1)} \end{bmatrix} \tag{A8}$$

are 3×3 matrices containing second derivatives of E (the double superscripts denote the two derivation variables, namely, $\underline{r}$ denotes the positional argument and ψ_1, ψ_2 the first and second angular arguments, respectively). Let us note that under the conditions (3.1),(3.2) the system is invariant under a translation of $\underline{R}_n$ and hence the elements (blocks) of the Hessian matrix depend (in addition to the sublattice indices γ, γ') only on the difference $n'-n$, so that they have been defined as $\underline{\underline{\mathbf{h}}}_{\gamma\gamma',n'-n}$. Let us also observe that the ground states found by the minimization procedure never display four different orientations but only two or one significant sublattices. The former subcase (only two distinguishable sublattices) corresponds to $\gamma=(0,0),(0,1)$ and $n=(n_1,n_2)$ with n_1 any integer and n_2 even integer, whereas the latter subcase (parallel molecules) corresponds to $\gamma=(0,0)$ and $n=(n_1,n_2)$ any pair of integers. In both cases the whole calculation is equivalent and in fact the Hessian matrix (A6) takes exactly the same form. Defining

$$\underline{\boldsymbol{\delta}}_{\gamma,n} \doteq \begin{bmatrix} \delta \underline{r}_{\gamma+n} \\ \delta \psi_{\gamma+n} \end{bmatrix}, \tag{A9}$$

the eigenvalue equation for the Hessian matrix can then be written as

$$\sum_{\gamma'} \sum_{n'} \underline{\underline{\mathbf{h}}}_{\gamma\gamma',n'-n} \cdot \underline{\boldsymbol{\delta}}_{\gamma',n'} = \lambda \underline{\boldsymbol{\delta}}_{\gamma,n}. \tag{A10}$$

Due to the dependence on $n'-n$ the left-hand side takes the form of a discrete convolution, which can be reduced to a product by means of a Fourier transform. Defining

$$\underline{\boldsymbol{\Delta}}_\gamma(\underline{k}) \doteq \sum_n \exp(-i\underline{k}\cdot\underline{R}_n)\, \underline{\boldsymbol{\delta}}_{\gamma,n}, \tag{A11}$$

$$\underline{\underline{\mathbf{H}}}_{\gamma\gamma'}(\underline{k}) \doteq \sum_n \exp(-i\underline{\underline{k}}\cdot\underline{\underline{R}}_n)\,\underline{\underline{\mathbf{h}}}_{\gamma\gamma',n}, \tag{A12}$$

we can easily write

$$\sum_{\gamma'} \underline{\underline{\mathbf{H}}}_{\gamma\gamma'}(-\underline{k})\cdot\underline{\boldsymbol{\Delta}}_{\gamma'}(\underline{k}) = \lambda\underline{\boldsymbol{\Delta}}_{\gamma}(\underline{k}), \tag{A13}$$

which is the eigenvalue equation for a $3s\times 3s$ matrix (s being the number of sublattices in which orientations have been found to be really different) depending on the ''wave vector'' $\underline{k}$. It is then possible to compute the eigenvalues of this matrix numerically, for $\underline{k}$ in the Brillouin zone associated with the Bravais lattice defined by $\underline{R}_n$, with a sufficient sampling density to verify the positivity of eigenvalues, as we have actually observed for the three phases described in the text.

[1] G. L. Gaines, Jr., *Insoluble Monolayers at Liquid-Gas Interfaces* (Interscience, New York, 1966).
[2] M. C. Petty, *Langmuir-Blodgett Films* (Cambridge University Press, Cambridge, 1996).
[3] *Physics of Amphiphilic Layers*, edited by J. Meunier, D. Langevin, and N. Boccara (Springer-Verlag, Berlin, 1987).
[4] *Micelles, Membranes, Microemulsion and Monolayers*, edited by W. M. Gelbart, A. Ben-Shaul, and D. Roux (Springer-Verlag, Berlin, 1994).
[5] C. M. Knobler and C. Desai, Annu. Rev. Phys. Chem. **43**, 207 (1992).
[6] V. M. Kaganer, H. Möhwald, and P. Dutta, Rev. Mod. Phys. **71**, 779 (1999).
[7] A. M. Bibo, C. M. Knobler, and I. R. Peterson, J. Phys. Chem. **95**, 5591 (1991).
[8] K. J. Strandburg, Rev. Mod. Phys. **60**, 161 (1988).
[9] H. Möhwald, Rep. Prog. Phys. **56**, 653 (1993).
[10] K. Kjaer, J. Als-Nielsen, C. A. Helm, L. A. Laxhuber, and H. Möwald, Phys. Rev. Lett. **58**, 2224 (1987).
[11] P. Dutta, J. B. Peng, B. Lin, J. B. Ketterson, M. Prakash, P. Georgopoulos, and S. Ehrlich, Phys. Rev. Lett. **58**, 2228 (1987).
[12] V. M. Kaganer, I. R. Peterson, R. M. Kenn, M. C. Shih, M. Durbin, and P. Dutta, J. Chem. Phys. **102**, 9412 (1995).
[13] I. Kuzmenko, V. M. Kaganer, and L. Leiserowitz, Langmuir **14**, 3882 (1998).
[14] A. I. Kitaigorodskii, *Organic Chemical Cristallography* (Consultants Bureau, New York, 1961).
[15] I. Weissbuch, M. Berfeld, W. Bouwman, K. Kjaer, J. Als-Nielsen, M. Lahav, and L. Leiserowitz, J. Am. Chem. Soc. **119**, 933 (1997).
[16] J. Hautman and M.L. Klein, J. Chem. Phys. **91**, 4994 (1989); **93**, 7483 (1990).
[17] D. R. Swanson, R. J. Hardy, and C. J. Eckhardt, J. Chem. Phys. **99**, 8194 (1993).
[18] M. D. Gibson, D. R. Swanson, C. J. Eckhardt, and X. C. Zeng, J. Chem. Phys. **106**, 1961 (1997).
[19] R. J. Meyer, Phys. Rev. A **12**, 1066 (1975); **13**, 1613 (1976).
[20] A. J. Berlinsky and A. B. Harris, Phys. Rev. Lett. **40**, 1579 (1978).
[21] A. B. Harris and A. J. Berlinsky, Can. J. Phys. **57**, 1852 (1979).
[22] E. Chacón and P. Tarazona, Phys. Rev. B **39**, 7111 (1989).
[23] L. Mederos, E. Chacón, and P. Tarazona, Phys. Rev. B **42**, 8571 (1990).
[24] P. Tarazona and E. Chacón, Phys. Rev. B **39**, 7157 (1989).
[25] O. G. Mouritsen and A. J. Berlinsky, Phys. Rev. Lett. **48**, 181 (1982).
[26] M. P. Allen and S. F. O'Shea, Mol. Simul. **1**, 47 (1987).
[27] Z.-X. Cai, Phys. Rev. B **43**, 6163 (1991).
[28] J. Schofield and S. A. Rice, J. Chem. Phys. **103**, 5792 (1995).
[29] D. R. Swanson, T. Luty, and C. J. Eckhardt, J. Chem. Phys. **107**, 4744 (1997).
[30] I. R. Peterson, R. M. Kenn, A. Goudot, P. Fontaine, F. Rondelez, W. G. Bouwman, and K. Kjaer, Phys. Rev. E **53**, 667 (1996).